

Article

Photodegradation of Decabrominated Diphenyl Ether in Soil Suspensions: Kinetics, Mechanisms and Intermediates

Kaibo Huang ^{1,2} , Haozhong Lin ³, Xueqin Tao ⁴, Mengyao Zou ⁴ and Guining Lu ^{2,3,*} ¹ School of Ecology and Environment, Hainan University, Haikou 570228, China; huangkaibo@hainanu.edu.cn² The Key Lab of Pollution Control and Ecosystem Restoration in Industry Clusters, Ministry of Education, South China University of Technology, Guangzhou 510006, China³ School of Environment and Energy, South China University of Technology, Guangzhou 510006, China; goolhz@163.com⁴ College of Resources and Environment, Zhongkai University of Agriculture and Engineering, Guangzhou 510225, China; xqtao_zhku@163.com (X.T.); mengyaozou_zhku@126.com (M.Z.)

* Correspondence: lutao@scut.edu.cn; Tel.: +86-20-3938-0569

Abstract: Pollution by polybrominated diphenyl ethers (PBDEs) is a major concern due to their bioaccumulation, persistence, and carcinogenicity. This study aimed to investigate the decabrominated diphenyl ether (BDE-209) photodegradation in soil suspensions. The results indicate BDE-209 can degrade in soil suspensions and its degradation follows pseudo-first-order kinetics. The light sources and intensity effects were studied and the photodegradation rates were 500 W Mercury Lamp > 300 W Mercury Lamp > 500 W Xenon Lamp > 300 W Xenon Lamp, which indicates UV light is the main reason for BDE-209 degradation. Soil particle inhibits BDE-209 photodegradation due to the light-shielding effect. BDE-209 photodegradation rates increased from 0.055 to 0.071 h⁻¹ with pH value increasing from 3.5 to 9.5. This may be because the products are more easily produced in higher pH soil suspensions. The presence of humic acid (HA) may inhibit BDE-209 photodegradation by photo-shielding. Fe³⁺ and Cu²⁺ have an adverse effect on BDE-209 photodegradation due to the photo competition. The •OH and ¹O₂ were detected in soil solutions. Analysis of the photoproducts of BDE-209 by gas chromatography mass spectrometry (GC-MS) and liquid chromatography time of flight mass spectrometry (LC-TOF-MS) showed that BDE-209 was mainly debrominated to the lower-brominated BDEs and the reactive oxygen radicals may not lead to BDE-209 degradation.

Keywords: BDE-209; soil suspension; photodegradation; products; mechanism

Citation: Huang, K.; Lin, H.; Tao, X.; Zou, M.; Lu, G. Photodegradation of Decabrominated Diphenyl Ether in Soil Suspensions: Kinetics, Mechanisms and Intermediates. *Processes* **2022**, *10*, 718. <https://doi.org/10.3390/pr10040718>

Academic Editor: Avelino Núñez-Delgado

Received: 23 March 2022

Accepted: 6 April 2022

Published: 8 April 2022

Publisher's Note: MDPI stays neutral with regard to jurisdictional claims in published maps and institutional affiliations.



Copyright: © 2022 by the authors. Licensee MDPI, Basel, Switzerland. This article is an open access article distributed under the terms and conditions of the Creative Commons Attribution (CC BY) license (<https://creativecommons.org/licenses/by/4.0/>).

1. Introduction

Polybrominated diphenyl ethers (PBDEs) are a class of halogenated organic pollutants including 209 homologues. Bromine atoms with strong reducibility can be dissociated at high temperature, and bromine atoms will capture the core free radicals of combustion reactions such as •OH and •O [1]. Because of its excellent flame retardant performance and high commercial value, it is often added as a flame retardant to the production of raw materials of electronic appliances, chemicals, and textiles [2]. Because most PBDEs are added to the product by physical addition, it is feasible to release them from the product to the environment [3–5]. Previous studies have reported they have detected PBDEs in air, water, soil, sediment, plant and animal tissue, and even human tissue [2,6–10]. Several researchers reported that PBDEs can cause reproductive toxicity, neurotoxicity, and endocrine system disruption [11–13]. Moreover, carcinogenic substances such as polybrominated dibenzofurans (PBDFs) and polybrominated dibenzo dioxins (PBDDs) will be produced in the processes of production, high-temperature pyrolysis, and natural reduction of PBDEs [14,15]. Therefore, it is necessary to examine the transformation of PBDEs in the environment.

Photodegradation is the main means of pollutant degradation in the environment [16]. Due to the absorption of ultraviolet light by PBDEs themselves, it becomes easier for PBDEs to be reduced by sunlight in the environment [17]. Therefore, PBDEs photo-transformation should attract significant attention. However, at present, most of the photochemical conversion of PBDEs is based on PBDE removal, thus ignoring the situation of PBDEs in the environment [18]. In addition, most studies have been conducted in the presence of organic solvents and catalysts, or have only studied low brominated PBDEs, ignoring the most widely used high brominated PBDEs on the market. Therefore, PBDEs should be explored under the condition of being closer to the natural environment.

PBDEs have strong hydrophobic properties, so they exist in the environment mainly via sorption on soil, sediment, and solid media [19,20]. Due to the strong light-shielding effect of soil particles, the lights decay when it irradiates deep soil. Therefore, it is difficult for PBDEs in deep soil to be photodegraded, and only PBDEs attached to the surface soil can be degraded [21]. However, in natural environments such as rivers, oceans, and farmland, PBDEs exist in solid suspension; thus, they can effectively absorb ultraviolet light and may degrade [18]. In addition, some studies have investigated the photodegradation of PBDEs on the solid surface [21,22], but few researchers have studied the photochemical process of PBDEs in soil suspension. Therefore, the photodegradation of PBDEs in soil suspension should be investigated.

As the most frequently detected and widely used congener of PBDEs, BDE-209 has attracted great attention in the past 20 years [13,22–24]. Therefore, BDE-209 was selected as a model pollutant. The kinetics of BDE-209 photodegradation with different light sources, and the effects of soil concentration, pH, and organic matter, were investigated. In addition, the products of BDE-209 were analyzed by GC-MS and LC-TOF-MS and the photodegradation pathway was proposed.

2. Materials and Methods

2.1. Materials

Humic acid (HA) (purity > 98%), 2,3-Dimethylpyridine-N-oxide (DMPO) (purity > 97%), and 2,2,6,6-Tetramethyl-1-piperidinyloxy (TEMP) (purity > 97%) were obtained from Sigma Chemical Co. (St. Louis, MO, USA). PBDE standards include BDE-209, 2,2',3,4,4',5',6-Heptabromodiphenyl ether (BDE-183), 2,2',4,4',5,6'-Hexabromodiphenyl ether (BDE-154), 2,2',4,4',5,5'-Hexabromodiphenyl ether (BDE-153), 2,2',4,4',6-Pentabromodiphenyl ether (BDE-100), 2,2',4,4',5-pentabromodiphenyl ether (BDE-99), 2,2',4,4'-trtribromodiphenyl ether (BDE-47), 2,4,4'-tribrominated diphenyl ether (BDE-28), 2,2',4-tribrominated diphenyl ether (BDE-17), 4,4'-dibrominated diphenyl ether (BDE-15), 2,4-dibrominated diphenyl ether (BDE-8), 2,4'-dibrominated diphenyl ether (BDE-7), 2,2'-dibrominated diphenyl ether (BDE-4), 4-brominated diphenyl ether (BDE-3), 2-brominated diphenyl ether (BDE-1), diphenyl ether (DE). The hydroxybiphenyl standards include ortho-hydroxybiphenyl (2-OH-DB) and para-hydroxybiphenyl (3-OH-DB). The brominated dibenzofuran standards are 2,8-dibrominated dibenzofuran (2,8-diBDF), 2,4-dibrominated dibenzofuran (2,4-diBDF), 2-brominated dibenzofuran (2-BDF), and dibenzofuran (DF). All these standards were obtained from AccuStandard, Inc. (New Haven, CT, USA). HPLC grade methanol, hexane, acetonitrile, isooctane, acetone, and tetrahydrofuran were obtained from CNW company (Shanghai, China). HCl and NaOH were purchased from Guangzhou Chemical Reagent Factory (Guangzhou, China). High purity nitrogen (99.999%) was purchased from Foshan Deli Messer Gas Co., Ltd. (Foshan, China).

2.2. BDE-209 Contaminated Soil and of Soil Suspension Preparation

BDE-209 contaminated soil preparation: Clean soil was prepared, and the weeds and branches were cleared in advance. Table 1 lists the physical and chemical properties of clean soil. Solutions of 1 L 1.0 and 2.0 g/L BDE-209 tetrahydrofuran were prepared. Two parts of 25.0 g clean soil without BDE-209 were weighed in beakers, to which were added 25 mL 1.0 g/L and 2.0 g/L BDE-209 solution, respectively. Then, the slurry was stirred

with a glass rod, placed in a ventilated kitchen at room temperature, avoiding light, and the solvent was volatilized. After 3 days, the 1.0 and 2.0 mg/g BDE-209 loaded contaminated soils were obtained. All the soil samples were kept in the refrigerator at $-20\text{ }^{\circ}\text{C}$ [25].

Table 1. The properties of background soils.

Contents	pH	SOM g/kg	Fe g/kg	H ₂ O %	CEC mmol/kg	Sand ¹ %	Silt ¹ %	Clay ¹ %
Soil	5.33	6.89	41.57	1.55	84.8	44.0	41.0	15.0

SOM: soil organic matter. CEC: cation exchange capacity. ¹: sand is the size of 2–0.05 mm, silt is the size of 0.05–0.002 mm, clay is the size of smaller than 0.002 mm.

Soil suspension preparation: A quantity of 0.02 g of BDE-209 contaminated soil was added to the tube, and then 15 mL of deionized water was added. The mixtures were stirred in the dark for 2 h, and then the soil suspensions containing BDE-209 were formed.

2.3. BDE-209 Photodegradation in Soil Suspension

The photodegradation processes were conducted in a BL-GHX-V photochemical reactor instrument Factory (Hasei Science Ins., Kaifeng, China). The reactor was equipped with a water-refrigerated high-pressure mercury or xenon lamp (300/500 W) to provide stable UV or simulated sunlight irradiation.

The 15 mL prepared soil suspension solutions were added to 22 mL foil-wrapped quartz tubes and a magnetic rotor was added at the same time. The tubes were placed in a photochemical reactor for stirring to reach equilibrium at $25 \pm 1\text{ }^{\circ}\text{C}$ for 2 h, which has been proven sufficient [26,27]. After the solutions reached equilibrium, the light was turned on for the photodegradation experiment. Samples were taken and determined at reaction times of 0, 0.5, 1, 3, 6, 9, 12, and 24 h, respectively. Three replicate samples were set at each time point under each experimental condition. The concentration of BDE-209 was determined by high performance liquid chromatography (HPLC), and the products were determined by GC-MS and LC-TOF-MS.

Under constant irradiation intensity, the photodegradation of BDE-209 was assumed to follow first-order kinetics:

$$C_t = C_0 e^{-kt} \quad (1)$$

where C_0 and C_t are the concentration of BDE-47 initially ($t = 0$ min) and at time t , respectively, and where k is the first-order rate constant (min^{-1}) [20,28].

2.4. Sample Pretreatment

The samples were centrifuged at the speed of 4000 r/min for 10 min to separate the solid and liquid phases. The liquid part was first used to determine the produced bromine ions, and then to detect BDE-209 and its degradation products in liquid. The solid part was extracted by adding 10 mL of acetone for 30 min, and then extracted by ultrasound for 30 min, during which the water temperature was maintained at $25\text{ }^{\circ}\text{C}$. The extracted solution was centrifuged at the speed of 3000 r/min for 5 min, and then the centrifuged liquid was filtered by a $0.22\text{ }\mu\text{m}$ PTFE filter membrane, the filtrate transferred to a 2 mL chromatographic bottle, and the content of BDE-209 was determined by HPLC. The recovery of BDE-209 in solid by this method was $83.5 \pm 2.5\%$. BDE-209 will not be degraded by the ultrasonic process. To the liquid separated from the suspension transfer to the glass centrifuge tube, 10 mL of n-hexane was added, before oscillation with a vortex oscillator for 5 min and ultrasonic treatment for 30 min. The organic phase was transferred to a new centrifuge tube and combined with the extraction liquid of the solid phase; this was blown gently with nitrogen gas until dry, and the volume was fixed with 1 mL of methanol in the chromatographic sample bottle. GC-MS and LC-TOF-MS were used to determine the possible non-polar and polar products produced in the reaction process [29].

2.5. Analytic Determination

HPLC analysis: The concentrations of BDE-209 were detected by Agilent 1260 high-performance liquid chromatography (HPLC) equipped with a UV detector. HPLC separation was performed on a Phenomenex C18 column (3.0 × 100 mm, 2.5 µm particle size). The mobile phase was acetonitrile/water (V/V, 95/5), and the flow rate was 1 mL/min. The injection volume was 20 µL. The column temperature was 27 ± 1 °C, and the retention time of BDE-209 was 12.0 ± 0.1 min. The results of the standard addition recovery test of the BDE-209 matrix showed that the standard addition recovery of BDE-209 was 85.3–103.7%; the detection limit was 0.10 µg/L and the limit of quantitation was 1.0 µg/L. The relative standard deviation (RSD) was 11%, meeting the requirements of BDE-209 detection in EPA1614 (EPA, 2007) (recovery range 50–200%, RSD less than 40%).

LC-TOF-MS analysis: The polar products were determined by LC-TOF-MS using an Agilent 1260 infinity HPLC system equipped with AB Sciex triple quadrupole TOF 5600 mass spectrometers. The mobile phase was 0.3% formic acid aqueous solution (a) and acetonitrile (b) at a flow rate of 0.2 mL/min. The samples were separated by Thermo BDS Hypersil C18 column (100 × 2.1 mm, 2.4 µm particles). The elution gradient procedure was: 10% B (0–4 min), 10–60% B (4–4.5 min, holding for 3 min), 60–80% B (7.5–8 min, holding for 3 min), 80–90% B (11–11.5 min, holding for 3.5 min), 90–100% B (15–15.5 min, holding for 9.5 min), and 100–10% B (25–25.5 min, holding for 9.5 min). The mass spectrometer operates under the negative ion mode using an electrospray ionization (ESI) source. The full scan (60–1000 *m/z*) ion spray voltage –4500 V was obtained under the following conditions—temperature: 550 °C, gas 1: 55 psi, gas 2: 55 psi, curtain gas: 35 psi, depolymerization potential: –80 V, collision energy: –10 V. Product ion scanning (MS/MS) was performed to obtain the fragmentation mode for structural analysis and change collision energy to optimize the sensitivity. During the analysis, the accuracy of MS and MS/MS data was determined by external quality calibration by inputting an APCI negative calibration solution into the instrument using an automatic calibration delivery system, and the calibration error was less than 3 ppm.

GC-MS analysis: Degradation products were analyzed using an Agilent Technologies (Santa Clara, CA, USA) 7890A GC coupled 5979C MSD GC-MS. The compounds were separated from a 15 m (id = 0.32 mm) capillary column (GAEQ-120318, ANPEL). The GC temperature was programmed from the initial temperature of 80 °C, increased to the final temperature of 300 °C at 10 °C/min, and maintained for 2 min, and then increased to 320 °C at 4 °C/min and maintained for 2 min. Helium was used as the carrier gas at a flow rate of 1.0 mL/min. The injection mode was the non-shunting mode, the ionization energy was 70 eV, the ion source temperature was 250 °C, and the 1.0 µL aliquot was injected into the syringe port maintained at 280 °C. The scanning methods were the full ion scanning method and the selective ion scanning method. The mass scanning range of full ion scanning was 60–1000 *m/z*. The mass scanning method of selective ion scanning was determined according to the peak time of existing standard samples and characteristic ions reported in the literature [14].

IC analysis: The concentration of bromine ions in aqueous solution was determined by ion chromatography, equipped with a double piston pump, Dionex DS6 conductivity detector, and Dionex IonPac AS14 analytical column (250 × 4 mm). The eluent (3.5 mM Na₂CO₃ and 1.0 mM NaHCO₃) was pumped at a flow rate of 1.0 mL/min and the injection volume was 20 µL. The suppressor current was 50 Ma, which was quantified by the standard curve external standard method.

ESR analysis: The content of instantaneous reactive oxygen species (¹O₂ and •OH) in the solution was semi-quantitatively determined by electron spin resonance spectroscopy (ESR). DMPO was used as the capture agent of •OH and TEMP was used as the capture agent of ¹O₂. The soil suspension solutions were irradiated by a 500 W mercury lamp, and the 1 mL sample was taken into the 1.5 mL sharp bottom tube containing 20 µL DMPO/TEMP after 10 min irradiation. The filtered solutions were detected by ESR. Under light conditions, the characteristic peaks of electron paramagnetic resonance spectroscopy

of the adducts of capture agent and reactive oxygen species TEMP- $^1\text{O}_2$ and DMPO-OH were measured, to determine whether $^1\text{O}_2$ and $\bullet\text{OH}$ are produced in the reaction system. The WINSIM software was used to fit the characteristic peak signal [25].

3. Results and Discussion

3.1. BDE-209 Photodegradation in Soil Suspensions

BDE-209 photodegradation under a 500 W mercury lamp, a 300 W mercury lamp, a 500 W xenon lamp, and a 300 W xenon lamp was investigated. As shown in Figure 1a, BDE-209 hardly degrades in the dark, which means BDE-209 may not be hydrolyzed in soil suspension. It can be degraded by 61.3% with 24 h of 500 W mercury lamp irradiation, and this achieved the fastest equilibrium within 12 h. BDE-209 degradation may have been uncompleted because some BDE-209 exists in the soil particle pores, which cannot absorb the light. The data within 12 h fitted well with the pseudo-first-order kinetic reaction, and the result is shown in Table 2. The light wavelength and intensity have a great influence on BDE-209 photodegradation in soil suspension. The BDE-209 photodegradation rate constants under the 500 W mercury lamp, 300 W mercury lamp, 500 W xenon lamp, and 300 W xenon lamp were 0.076, 0.036, 0.013, and 0.010 h^{-1} respectively, and the corresponding photodegradation half-lives were 9.079, 18.809, 52.750, and 69.038 h, respectively. These indicate that ultraviolet light is the key to BDE-209 degradation, which is mainly due to the absorption of BDE-209 in the ultraviolet band.

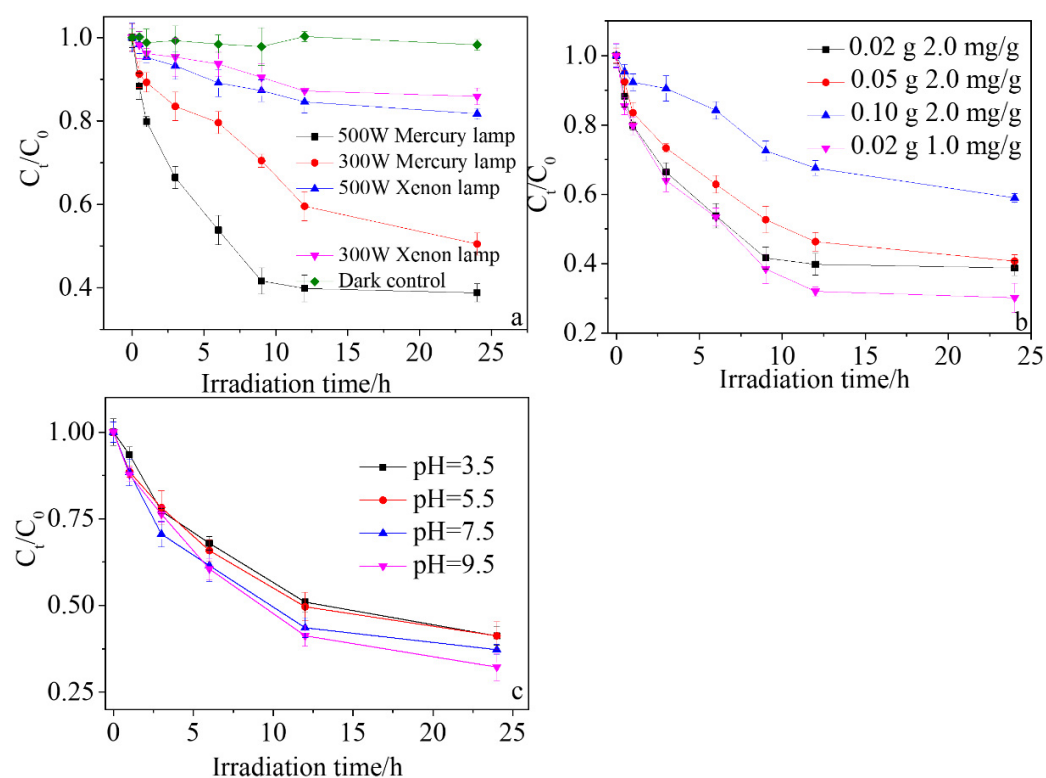


Figure 1. BDE-209 photodegradation in soil suspensions under: (a) different light sources; (b) different initial concentrations; (c) different pH values.

Table 2. BDE-209 photolysis kinetic parameters with different light sources.

Light Source	BDE-209/Soil (mg/g)	$t_{1/2}$ (h)	k_p (h^{-1})	R^2
500 W mercury lamp	2	9.079	0.076	0.9407
300 W mercury lamp	2	18.809	0.036	0.9502
500 W Xenon lamp	2	52.750	0.013	0.9371
300 W Xenon lamp	2	69.038	0.010	0.9525

Using a 500 W mercury lamp as a light source, the photodegradation experiments were carried out with 0.02, 0.05, and 0.10 g of 2 mg/g BDE-209 and 0.02 g of 1 mg/g BDE-209 samples, respectively. The results are shown in Figure 1b and the fitted kinetic parameters are listed in Table 3. Compared with the addition of 0.02 g, the photodegradation rate of BDE-209 will significantly slow down with the soil additions of 0.05 and 0.10 g; the photodegradation rate constants decrease from 0.076 to 0.061 and 0.031 h^{-1} , and the half-life increases from 9.079 h to 11.301 and 22.323 h, respectively. This may be because of the shielding effect of soil particles on the light. With the increase in soil particles, the irradiation of the light source in the system is hindered, the photons absorbed by BDE-209 are reduced, and the degradation reaction is slowed. Moreover, for the 0.02 g soil addition, the photodegradation rate of 1 mg/g BDE-209 was faster than that of 2 mg/g. This may be attributed to the competition between molecules at high concentrations.

Table 3. BDE-209 photolysis kinetic parameters under different initial concentrations.

BDE-209/Soil (mg/g)	Amount (g)	$t_{1/2}$ (h)	k_p (h^{-1})	R^2
2	0.02	9.079	0.076	0.9407
2	0.05	11.301	0.061	0.9682
2	0.10	22.323	0.031	0.9695
1	0.02	7.672	0.090	0.9763

The pH value of the reaction system usually has a great impact on the photochemical degradation rate of organic compounds. The photodegradation experiment was conducted with a 500 W mercury lamp, and phosphate was selected as a buffer solution; the soil solutions' pH values were adjusted to 3.5, 5.5, 7.5, and 9.5 by NaOH and HCl. As shown in Figure 1c and Table 4, with the increase in the pH values from 3.5 to 9.5, the degradation rate increased from 0.055 to 0.071 h^{-1} . This is consistent with the previous research results [30]; this result may be because protons are the main product of BDE-209 degradation, and a higher pH level can support more hydroxide ions to neutralize the generated protons to promote the forward reaction by weakening the proton effect.

Table 4. Photolysis kinetic parameters of BDE-209 in soil suspensions under different pH values.

BDE-209/Soil (mg/g)	pH Value	$t_{1/2}$ (h)	k_p (h^{-1})	R^2
2	3.5	12.543	0.055	0.9721
2	5.5	12.340	0.056	0.9779
2	7.5	10.445	0.066	0.9596
2	9.5	9.628	0.071	0.9907

3.2. The Effect of HA on BDE-209 Photodegradation in Soil Suspensions

Humic acid (HA) is a kind of common organic matter in the natural environment, and is widely distributed in soil and natural water. It contains a large number of chromogenic groups such as hydroxyl, carboxyl, carbonyl, and benzene rings. It can act as a photosensitive compound or a photoactive substance in the environment during light

irradiation. It can absorb ultraviolet light at a certain wavelength, thus affecting the photochemical process. Relevant study shows that, in addition to the light-shielding effect, HA can also quench the excited state of pollutants, which may also inhibit the photolysis of pollutants [31].

The 0, 5, and 10 mg/L HA soil solutions containing BDE-209 were irradiated with a 500 W mercury lamp. The results shown in Figure 2 and the photodegradation kinetics data are listed in Table 5. As shown in Figure 2, HA has a strong inhibitory effect on the photodegradation of BDE-209 at a certain concentration. When the HA concentration increased from 0 to 10 mg/L, the BDE-209 degradation rate decreased from 0.072 to 0.024 h⁻¹, and the half-life increased from 9.627 to 28.881 h. This may be due to: (1) the BDE-209 molecule being wrapped by the HA macromolecule, which hinders the intermolecular reaction; (2) HA absorbs ultraviolet light and competes with BDE-209 to absorb photons, and light shielding reduces the absorption efficiency of BDE-209 for ultraviolet light and slows the degradation rate; and (3) HA competes with BDE-209 to bind reactive oxygen species (ROS) and quench the excited BDE-209 at the same time, to inhibit the photodegradation of BDE-209 in the soil water suspension.

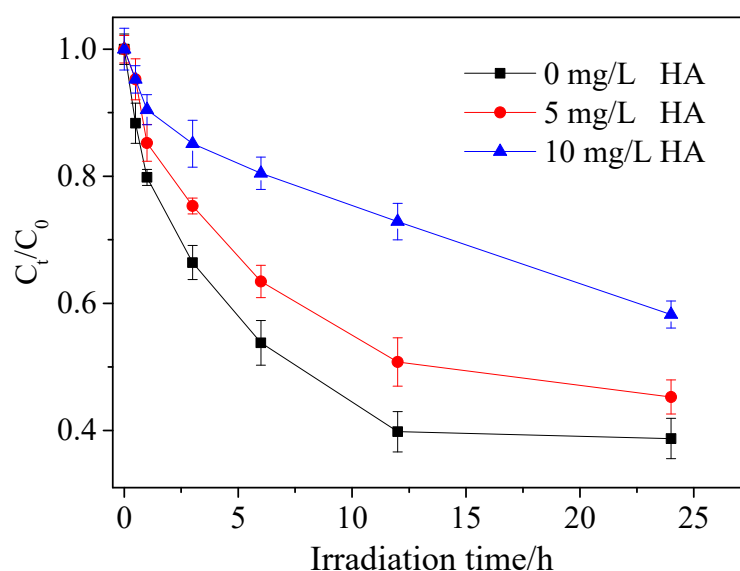


Figure 2. BDE-209 photodegradation in soil suspensions under different concentrations of HA.

Table 5. BDE-209 photodegradation kinetic parameters with different concentrations of HA.

BDE-209/Soil (mg/g)	HA (mg/L)	$t_{1/2}$ (h)	k_p (h ⁻¹)	R^2
2	0	9.627	0.072	0.9355
2	5	12.836	0.054	0.9387
2	10	28.881	0.024	0.8902

3.3. The Effect of HA on BDE-209 Photodegradation in Soil Suspensions

In PBDE-polluted areas, there is usually serious heavy metal contamination. Previous researchers reported that PBDEs and some heavy metals (Cu²⁺ and Zn²⁺) have simultaneously been detected in the environment [32], and that ferric ions also exist [33]. Moreover, Fe³⁺, Cu²⁺, and Zn²⁺ have certain photochemical activities that can stimulate the generation of ROS in aqueous solution and oxidize organic pollutants [33,34]. Therefore, it is necessary to investigate the effects of Fe³⁺, Cu²⁺, and Zn²⁺ on BDE-209 photodegradation in soil suspensions.

The effects of the three ions are shown in Figure 3b–d, and the kinetic parameters are listed in Table 6. The results indicate that they all hindered the BDE-209 photodegradation

in soil suspensions, and with the increase in the Fe^{3+} , Cu^{2+} , and Zn^{2+} ions' concentration from 0 to 1 mM, the BDE-209 degradation rates decreased from 0.035 to 0.013, 0.023, and 0.030 h^{-1} , respectively. This may be because Fe^{3+} , Cu^{2+} , and Zn^{2+} have absorbance in the wavelength of 190–400 nm, which is shown in Figure 3a. Therefore, the metal ions may act as photo competitors to inhibit the BDE-209 degradation. Moreover, we also found the UV absorption wavelength range of Fe^{3+} is the widest, Cu^{2+} has strong absorption near the wavelength of 240 nm, and Zn^{2+} has weak UV absorption; thus, Fe^{3+} has the greatest effect and Zn^{2+} is the weakest.

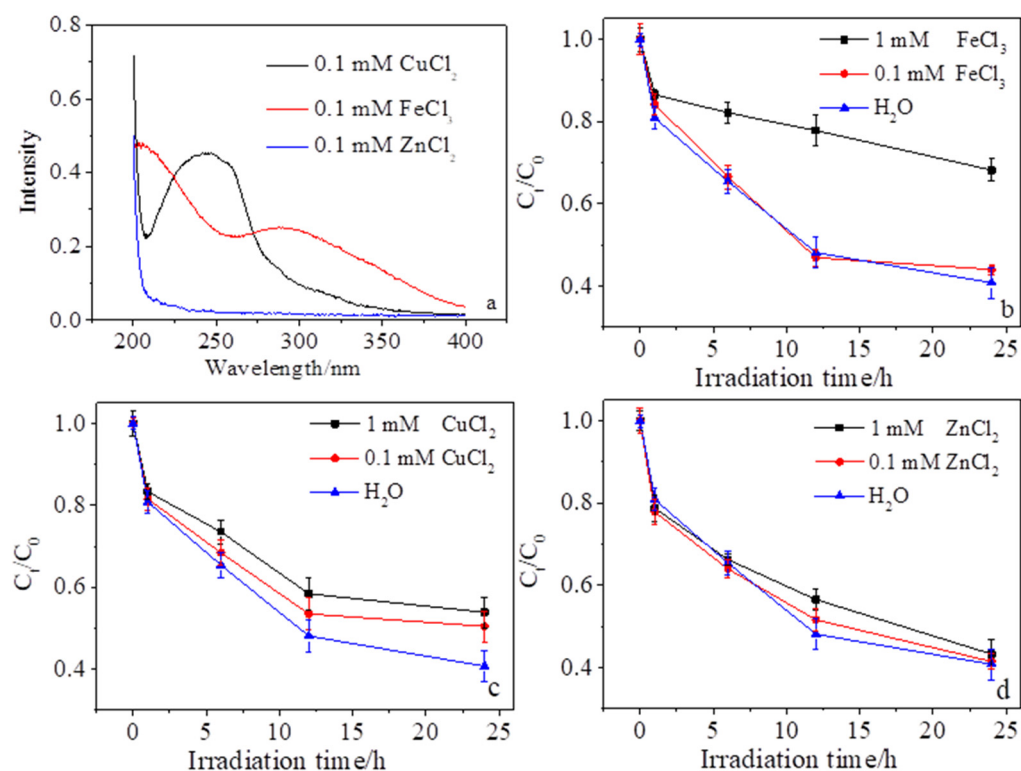


Figure 3. (a) UV absorption spectrum of 0.1 mM FeCl_3 , CuCl_2 and ZnCl_2 solution; BDE-209 photodegradation in soil suspensions with different FeCl_3 (b), CuCl_2 (c) and ZnCl_2 (d) solutions.

Table 6. BDE-209 photodegradation kinetic parameters with different metal ions solutions.

BDE-209/Soil (mg/g)	Metal Ions	$t_{1/2}$ (h)	k_p (h^{-1})	R^2
2	Water	19.736	0.035	0.8462
2	1 mM FeCl_3	52.194	0.013	0.8180
2	0.1 mM FeCl_3	20.852	0.033	0.7777
2	1 mM CuCl_2	29.259	0.023	0.7906
2	0.1 mM CuCl_2	26.496	0.026	0.7427
2	1 mM ZnCl_2	22.410	0.030	0.8791
2	0.1 mM ZnCl_2	21.023	0.032	0.8513

The radicals in the soil suspensions with Fe^{3+} , Cu^{2+} , and Zn^{2+} ions were detected by ESR, and showed that $\bullet\text{OH}$ and $^1\text{O}_2$ exist in the reaction system, as shown in Figure 4. However, the large abundance of organic matter may quench these radicals, resulting in the radicals formed by metals ions having a little effect on the BDE-209 degradation. In addition, previous studies reported that the BDE-209 is hardly attacked by the radicals as the full bromine exists on the two-benzene ring [35]. The lack of BDE-209 oxidation products in the LC-TOF-MS results also proves this. This may result in the radical being unable to directly influence the BDE-209 degradation. Therefore, the $\text{OH}\bullet$ and $^1\text{O}_2$ produced

by metals cannot accelerate the BDE-209 degradation, and the metals can only affect BDE-209 photodegradation in the soil solution by photo competition, thereby inhibiting the degradation.

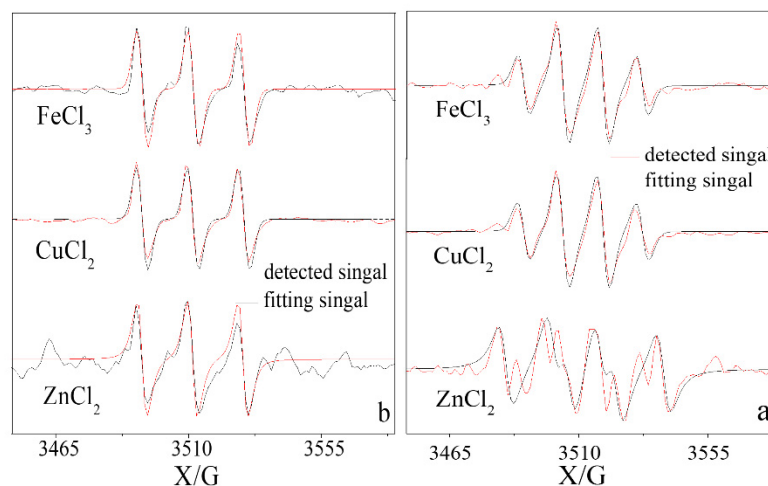


Figure 4. ESR spectra for 0.1 mM metal ion solution: (a) $\bullet\text{OH}$ and (b) $^1\text{O}_2$.

3.4. The Products of BDE-209 Degradation in Soil Suspensions

The products of BDE-209 photodegradation in soil suspension were detected and the results indicate that BDE-209 may mainly undergo a debromination process, which is consistent with the previous research results [35]. Due to the absence of the standards, we only identified the products of BDE-183, BDE-154, BDE-153, BDE-100, BDE-99, BDE-47, BDE-28, and BDE-15 in the full scan chromatogram of BDE-209 photodegradation (Figure 5a). Moreover, the Br^- in the photodegradation solution was monitored by ion chromatography (IC), and indicated the production of bromine ion is consistent with the degradation of BDE-209 (Figure 5b). They all reached equilibrium within 12 h. However, there was no match between the BDE-209 degradation amount and the production of Br^- , and the Br^- concentration was between the removal of only one bromine and full bromine removal. This may be because (1) many intermediates accumulated during the degradation of BDE-209, and (2) bromine removed during BDE-209 degradation generates bromate ions.

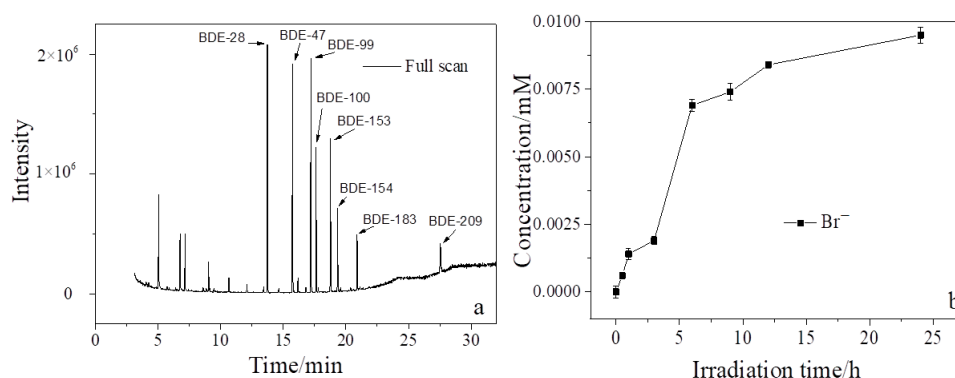


Figure 5. (a) GC-MS chromatograms of BDE-209 photodegradation; (b) the concentration of bromide ions in the reaction system.

The accumulation of low brominated PBDE products was found by detecting BDE-209 samples with different degradation times, as shown in Figure 6. The debromination product of BDE-209 with 2–9 bromine was justified by mass spectrometry and the degree of bromination of the detected products decreased with the UV irradiation time. This indicates BDE-209 underwent a step-by-step debromination process. In addition, each

product has many homologues, which means the BDE-209 and its products have multiple reaction pathways.

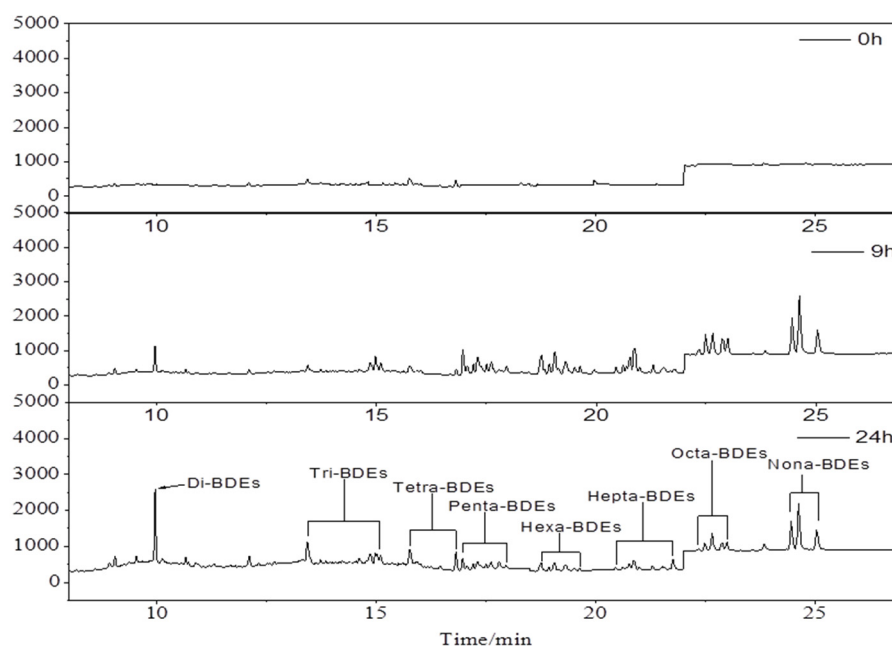


Figure 6. The products of BDE-209 in soil suspension after photodegradation.

Previous studies showed that polybrominated dibenzofurans (PBDFs) are formed during photodegradation [25]. However, we did not find the formation of PBDFs in GC-MS full scan chromatography. This may be because the organic matter quenches the excited state of BDE-209 to hinder the formation of PBDFs by intermolecular reaction. In addition, since the characteristic peak signals of $\text{OH}\cdot$ and $^1\text{O}_2$ were detected in the reaction system, we speculate that oxidation products or hydroxylation products may be generated, but the detection results of LC-TOF-MS show no relevant products were found in the experiment. The photodegradation mechanism of BDE-209 in the soil water suspension is mainly due to the direct debromination, which produces low brominated diphenyl ethers. In conclusion, the photodegradation path of BDE-209 in soil suspension is drawn in Figure 7.

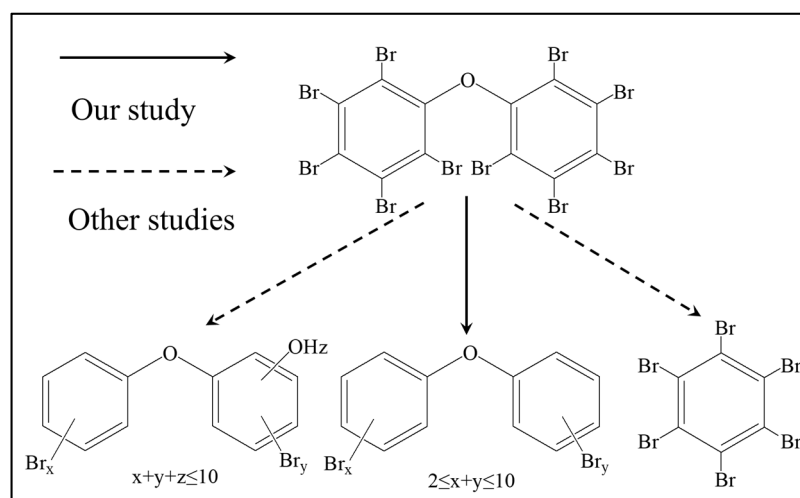


Figure 7. The photodegradation pathways of BDE-209 in soil suspensions.

4. Conclusions

In this study, the photodegradation of BDE-209 in soil suspensions was studied to investigate the transformation of PBDEs in the environment during solar irradiation. The results showed that BDE-209 can be degraded by UV irradiation in soil solution and followed pseudo-first-order kinetics within 12 h. The light wavelength and intensity have a great influence on BDE-209 photodegradation in soil suspension, and UV light is the key to the BDE-209 degradation. The light-shielding effect of soil particles can inhibit the BDE-209 photodegradation. With the increase in the pH value, the BDE-209 photodegradation increased. Light shielding and quenching of active substances are the main reasons HA inhibited the photodegradation of BDE-209 in soil suspension. Although the metals can produce radicals, they can only affect BDE-209 photodegradation in soil solution by photo competition, thereby inhibiting the degradation. The products of BDE-209 were analyzed and showed that it mainly undergoes a step-by-step debromination process, and no oxidation products were detected. The above experimental results provide a basis for the photochemical transformation of BDE-209 in soil suspension. In addition, our research was not conducted in a natural environmental; in the future, the photochemical transformation process of PBDE-contaminated soil suspension by sunlight irradiation should be explored.

Author Contributions: K.H.: Conceptualization, Methodology, Validation, Formal analysis, Data Curation, Writing—Original Draft, Visualization, Writing—Review and Editing. H.L.: Formal analysis, Data Curation, Writing—Review and Editing. X.T. and M.Z.: Conceptualization: G.L.: Conceptualization; Supervision; Project administration; Funding acquisition. All authors have read and agreed to the published version of the manuscript.

Funding: This work was financially supported by the National Natural Science Foundation of China (No. 42077114) and the Guangdong Science and Technology Program (2020B121201003) and Guangdong Special Support Program for Local Innovative and Research Teams Project (No. 2019BT02L218).

Institutional Review Board Statement: Not applicable.

Informed Consent Statement: Not applicable.

Data Availability Statement: Not applicable.

Conflicts of Interest: The authors declare no conflict of interest.

References

1. Bu, Q.; Wu, D.; Xia, J.; Wu, M.; Liu, X.; Cao, Z.; Yu, G. Polybrominated diphenyl ethers and novel brominated flame retardants in indoor dust of different microenvironments in Beijing, China. *Environ. Int.* **2019**, *122*, 159–167. [[CrossRef](#)] [[PubMed](#)]
2. Wu, Z.; Han, W.; Yang, X.; Li, Y.; Wang, Y. The occurrence of polybrominated diphenyl ether (PBDE) contamination in soil, water/sediment, and air. *Environ. Sci. Pollut. Res.* **2019**, *26*, 23219–23241. [[CrossRef](#)] [[PubMed](#)]
3. Abbasi, G.; Buser, A.M.; Soehl, A.; Murray, M.W.; Diamond, M.L. Stocks and Flows of PBDEs in Products from Use to Waste in the US and Canada from 1970 to 2020. *Environ. Sci. Technol.* **2015**, *49*, 1521–1528. [[CrossRef](#)] [[PubMed](#)]
4. Hahladakis, J.N.; Velis, C.A.; Weber, R.; Iacovidou, E.; Purnell, P. An overview of chemical additives present in plastics: Migration, release, fate and environmental impact during their use, disposal and recycling. *J. Hazard. Mater.* **2018**, *344*, 179–199. [[CrossRef](#)]
5. Huang, K.; Guo, J.; Xu, Z. Recycling of waste printed circuit boards: A review of current technologies and treatment status in China. *J. Hazard. Mater.* **2009**, *164*, 399–408. [[CrossRef](#)]
6. Cequier, E.; Ionas, A.C.; Covaci, A.; Maria Marce, R.; Becher, G.; Thomsen, C. Occurrence of a Broad Range of Legacy and Emerging Flame Retardants in Indoor Environments in Norway. *Environ. Sci. Technol.* **2014**, *48*, 6827–6835. [[CrossRef](#)]
7. Darnerud, P. Toxic effects of brominated flame retardants in man and in wildlife. *Environ. Int.* **2003**, *29*, 841–853. [[CrossRef](#)]
8. De Wit, C.A. An overview of brominated flame retardants in the environment. *Chemosphere* **2002**, *46*, 583–624. [[CrossRef](#)]
9. Giulivo, M.; Capri, E.; Kalogianni, E.; Milacic, R.; Majone, B.; Ferrari, F.; Eljarrat, E.; Barcelo, D. Occurrence of halogenated and organophosphate flame retardants in sediment and fish samples from three European river basins. *Sci. Total Environ.* **2017**, *586*, 782–791. [[CrossRef](#)]
10. Shen, M.; Ge, J.; Lam, J.C.W.; Zhu, M.; Li, J.; Zeng, L. Occurrence of two novel triazine-based flame retardants in an E-waste recycling area in South China: Implication for human exposure. *Sci. Total Environ.* **2019**, *683*, 249–257. [[CrossRef](#)]

11. Bonde, J.P.; Flachs, E.M.; Rimborg, S.; Glazer, C.H.; Giwercman, A.; Ramlau-Hansen, C.H.; Hougaard, K.S.; Hoyer, B.B.; Haervig, K.K.; Petersen, S.B.; et al. The epidemiologic evidence linking prenatal and postnatal exposure to endocrine disrupting chemicals with male reproductive disorders: A systematic review and meta-analysis. *Hum. Reprod. Update* **2017**, *23*, 104–125. [[CrossRef](#)] [[PubMed](#)]
12. Boas, M.; Feldt-Rasmussen, U.; Main, K.M. Thyroid effects of endocrine disrupting chemicals. *Mol. Cell. Endocrinol.* **2012**, *355*, 240–248. [[CrossRef](#)] [[PubMed](#)]
13. Costa, L.G.; de Laat, R.; Tagliaferri, S.; Pellacani, C. A mechanistic view of polybrominated diphenyl ether (PBDE) developmental neurotoxicity. *Toxicol. Lett.* **2014**, *230*, 282–294. [[CrossRef](#)] [[PubMed](#)]
14. Liang, J.; Lu, G.; Wang, R.; Tang, T.; Huang, K.; Jiang, F.; Yu, W.; Tao, X.; Yin, H.; Dang, Z. The formation pathways of polybrominated dibenzo-p-dioxins and dibenzofurans (PBDD/Fs) from pyrolysis of polybrominated diphenyl ethers (PBDEs): Effects of bromination arrangement and level. *J. Hazard. Mater.* **2020**, *399*, 123004. [[CrossRef](#)] [[PubMed](#)]
15. Wang, R.; Tang, T.; Xie, J.; Tao, X.; Huang, K.; Zou, M.; Yin, H.; Dang, Z.; Lu, G. Debromination of polybrominated diphenyl ethers (PBDEs) and their conversion to polybrominated dibenzofurans (PBDFs) by UV light: Mechanisms and pathways. *J. Hazard. Mater.* **2018**, *354*, 1–7. [[CrossRef](#)]
16. Kurtz, T.; Zeng, T.; Rosario-Ortiz, F.L. Photodegradation of cyanotoxins in surface waters. *Water Res.* **2021**, *192*, 116804. [[CrossRef](#)]
17. Rodenburg, L.A.; Meng, Q.; Yee, D.; Greenfield, B.K. Evidence for photochemical and microbial debromination of polybrominated diphenyl ether flame retardants in San Francisco Bay sediment. *Chemosphere* **2014**, *106*, 36–43. [[CrossRef](#)]
18. Pan, Y.; Tsang, D.C.; Wang, Y.; Li, Y.; Yang, X. The photodegradation of polybrominated diphenyl ethers (PBDEs) in various environmental matrices: Kinetics and mechanisms. *Chem. Eng. J.* **2016**, *297*, 74–96. [[CrossRef](#)]
19. Santos, M.S.; Alves, A.; Madeira, L.M. Chemical and photochemical degradation of polybrominated diphenyl ethers in liquid systems—A review. *Water Res.* **2016**, *88*, 39–59. [[CrossRef](#)]
20. Huang, K.; Lu, G.; Zheng, Z.; Wang, R.; Tang, T.; Tao, X.; Cai, R.; Dang, Z.; Wu, P.; Yin, H. Photodegradation of 2,4,4'-tribrominated diphenyl ether in various surfactant solutions: Kinetics, mechanisms and intermediates. *Environ. Sci. Processes Impacts* **2018**, *20*, 806–812. [[CrossRef](#)]
21. Hua, I.; Kang, N.; Jafvert, C.T.; Fábrega-Duque, J.R. Heterogeneous photochemical reactions of decabromodiphenyl ether. *Environ. Toxicol. Chem. Int. J.* **2003**, *22*, 798–804. [[CrossRef](#)]
22. Ahn, M.; Filley, T.; Jafvert, C.; Nies, L.; Hua, I.; Bezares-Cruz, J. Photodegradation of Decabromodiphenyl Ether Adsorbed onto Clay Minerals, Metal Oxides, and Sediment. *Environ. Sci. Technol.* **2006**, *40*, 215–220. [[CrossRef](#)] [[PubMed](#)]
23. Wang, R.; Lu, G.; Lin, H.; Huang, K.; Tang, T.; Xue, X.; Yang, X.; Yin, H.; Dang, Z. Relative roles of H-atom transfer and electron transfer in the debromination of polybrominated diphenyl ethers by palladized nanoscale zerovalent iron. *Environ. Pollut.* **2016**, *222*, 331–337. [[CrossRef](#)] [[PubMed](#)]
24. Zhang, S.; Xu, X.; Wu, Y.; Ge, J.; Li, W.; Huo, X. Polybrominated diphenyl ethers in residential and agricultural soils from an electronic waste polluted region in South China: Distribution, compositional profile, and sources. *Chemosphere* **2014**, *102*, 55–60. [[CrossRef](#)] [[PubMed](#)]
25. Huang, K.; Liu, H.; He, J.; Li, Y.; Wang, R.; Tang, T.; Tao, X.; Yin, H.; Dang, Z.; Lu, G. Photoassisted degradation of 2,2',4,4'-tetrabrominated diphenyl ether in simulated soil washing system containing Triton X series surfactants. *Environ. Pollut.* **2020**, *265*, 115005. [[CrossRef](#)] [[PubMed](#)]
26. Tang, L.; Wang, J.; Zeng, G.; Liu, Y.; Deng, Y.; Zhou, Y.; Tang, J.; Wang, J.; Guo, Z. Enhanced photocatalytic degradation of norfloxacin in aqueous Bi₂WO₆ dispersions containing nonionic surfactant under visible light irradiation. *J. Hazard. Mater.* **2016**, *306* (Suppl. C), 295–304. [[CrossRef](#)] [[PubMed](#)]
27. Liu, J.W.; Han, R.; Wang, H.T.; Zhao, Y.; Chu, Z.; Wu, H.Y. Photoassisted degradation of pentachlorophenol in a simulated soil washing system containing nonionic surfactant Triton X-100 with La–B codoped TiO₂ under visible and solar light irradiation. *Appl. Catal. B Environ.* **2011**, *103*, 470–478. [[CrossRef](#)]
28. Wang, R.; Tang, T.; Wei, Y.; Dang, D.; Huang, K.; Chen, X.; Yin, H.; Tao, X.; Lin, Z.; Dang, Z.; et al. Photocatalytic debromination of polybrominated diphenyl ethers (PBDEs) on metal doped TiO₂ nanocomposites: Mechanisms and pathways. *Environ. Int.* **2019**, *127*, 5–12. [[CrossRef](#)]
29. Huang, K.; Liu, H.; He, J.; He, Y.; Tao, X.; Yin, H.; Dang, Z.; Lu, G. Application of Ag/TiO₂ in photocatalytic degradation of 2,2',4,4'-tetrabromodiphenyl ether in simulated washing waste containing Triton X-100. *J. Environ. Chem. Eng.* **2021**, *9*, 105077. [[CrossRef](#)]
30. Huang, K.; Lu, G.; Lian, W.; Xu, Y.; Wang, R.; Tang, T.; Tao, X.; Yi, X.; Dang, Z.; Yin, H. Photodegradation of 4,4'-dibrominated diphenyl ether in Triton X-100 micellar solution. *Chemosphere* **2017**, *180*, 423–429. [[CrossRef](#)]
31. Wu, D.; Li, M.; Du, L.; Ren, D.; Wang, J. Straw return in paddy field alters photodegradation of organic contaminants by changing the quantity rather than the quality of water-soluble soil organic matter. *Sci. Total Environ.* **2022**, *821*, 153371. [[CrossRef](#)] [[PubMed](#)]
32. Moeckel, C.; Breivik, K.; Nøst, T.H.; Sankoh, A.; Jones, K.C.; Sweetman, A. Soil pollution at a major West African E-waste recycling site: Contamination pathways and implications for potential mitigation strategies. *Environ. Int.* **2020**, *137*, 105563. [[CrossRef](#)] [[PubMed](#)]
33. Huang, K.; Liang, J.; Jafvert, C.T.; Li, Q.; Chen, S.; Tao, X.; Zou, M.; Dang, Z.; Lu, G. Effects of ferric ion on the photo-treatment of nonionic surfactant Brij35 washing waste containing 2,2',4,4'-terabromodiphenyl ether. *J. Hazard. Mater.* **2021**, *415*, 125572. [[CrossRef](#)]

34. Hu, J.; Chen, H.; Hou, X.; Jiang, X. Cobalt and Copper Ions Synergistically Enhanced Photochemical Vapor Generation of Molybdenum: Mechanism Study and Analysis of Water Samples. *Anal. Chem.* **2019**, *91*, 5938–5944. [[CrossRef](#)] [[PubMed](#)]
35. Panda, D.; Manickam, S. Heterogeneous Sono-Fenton treatment of decabromodiphenyl ether (BDE-209): Debromination mechanism and transformation pathways. *Sep. Purif. Technol.* **2019**, *209*, 914–920. [[CrossRef](#)]